

DISPERSION OF AIR IN THE REGION

2000A to 7000A.

W. D. Komhyr.

For Reference

NOT TO BE TAKEN FROM THIS ROOM

Ex LIBRIS
UNIVERSITATIS
ALBERTAENSIS



56(F)
19

UNIVERSITY OF ALBERTA

"Dispersion of Air in the Region 2000 Å to 7000 Å"

A DISSERTATION

SUBMITTED TO THE SCHOOL OF GRADUATE STUDIES
IN PARTIAL FULFILMENT OF THE REQUIREMENTS FOR THE DEGREE
OF MASTER OF SCIENCE

FACULTY OF ARTS AND SCIENCE

DEPARTMENT OF PHYSICS

by


WALTER DMYTRO KOMHYR

Edmonton - Alberta

ABSTRACT

The well known interference method devised by Fabry and Buisson⁽¹⁾ has been employed in determining two relative dispersion curves of different forms, for dry, carbon dioxide-free air in the wavelength range 2536 Å to 6266 Å. The method uses an interferometer interposed between an achromatic lens and a condensing lens near which is positioned a light source in a manner such that resulting Haidinger fringes are focussed on the slit of a spectrograph. Light sources utilized were an electrodeless $^{198}_{80}\text{Hg}$. lamp which emitted radiations free from isotope shifts and hyperfine structure, and a neon secondary standard lamp. The relative curves were adjusted to normal conditions (15 °C and 860 mm. of mercury pressure) by obtaining a 'best fit' with values of refractive index in the visible region calculated from averaged data of Barrell and Sears, and of Perard (see Appendix D). The resulting curves were finally corrected to standard air which contains 0.03% carbon dioxide.

Incidental to the main problem under investigation was a study of the effect of air pressure on a Fabry Perot etalon. It has been pointed out⁽²⁾ that pressure corrections hitherto based on the compression of the etalon spacer material alone might need some revision.



Digitized by the Internet Archive
in 2018 with funding from
University of Alberta Libraries

<https://archive.org/details/komhyr1956>

TABLE OF CONTENTS

I	INTRODUCTION	1
II	THEORY	
	1. Theory of Refractive Index	4
	2. The Fabry Perot Interferometer	5
	3. Determination of Refractive Index of Air	9
	4. Phase Change on Reflection	11
III	APPARATUS AND EXPERIMENTAL PROCEDURE	
	1. Optical Apparatus	13
	2. Light Sources and Excitation	16
	3. Vacuum - Air System	17
	4. Constant Temperature Bath	20
	5. The Densitometer	21
	6. Procedure in Taking Exposures	23
	i Vacuum Exposures	
	ii Air Exposures	
IV	RESULTS AND DISCUSSION	
	1. Effect of Air Pressure on the Etalon	26
	2. Dispersion Curves for Air	28

APPENDIX A Calibration of the Beckmann Thermometer

APPENDIX B Horizontal Focus of the Spectrograph

APPENDIX C Method of Least Squares

APPENDIX D Reduction of Relative Dispersion Equations
to Standard Conditions, and of Neon Standards
to Exposure Conditions.

APPENDIX E Observed Data

LIST OF PLATES AND FIGURES

	Following Page
Fig. 1 Multiple Beam Transmitting Interferometer	5
Fig. 2 General Arrangement of Optical Apparatus	14
Fig. 3 Schematic Diagram of Apparatus Used in Measuring Etalon Chamber Pressures	17
Fig. 4 Photomultiplier Circuit	21
Fig. 5 Cross-section of Vertical Type Etalon	28
Fig. 6 Manometer Used in Calibrating the Beckmann Thermometer	
PLATE I An Unassembled Fabry Perot Etalon	13
PLATE II General View of the Apparatus	15
PLATE III The Recording Densitometer	20
PLATE IV Some Interferograms From A Typical Plate	22
PLATE V Typical Tracings of Fabry Perot Interference Fringes	24

I INTRODUCTION

Original inquiries into the refractivity of air stemmed from a need to correct astronomical observations for the refraction of the earth's atmosphere. More recently, spectroscopists have been concerned with the determination of atomic and molecular energy levels from wavelength measurements usually performed more conveniently in air rather than vacuum. Since the energy relations must be expressed in vacuum wave numbers, wavelengths as determined in air are multiplied by appropriate indices of refraction in order to convert them to vacuum values. At present, measurements of wavelength are being made to 8 significant figures, corresponding to an accuracy approaching 1 part in 10^8 at 10,000 Å. It is necessary, therefore, to know refractive index to the same precision.

One of the first major investigations of the dispersion of air was undertaken in 1918 at the National Bureau of Standards by Meggers and Peters⁽³⁾ who expressed their results in terms of the refractivity of dry air containing an unspecified amount of carbon dioxide at 0°C, 15°C and 30°C, and 760 mm. of mercury pressure. Their observations in the spectral range 2218 Å to 8999 Å were satisfactorily represented (except for a slight deviation in the red) by the empirical Cauchy formula

$$n - 1 = a + \frac{b}{\lambda^2} + \frac{c}{\lambda^4} \quad (1)$$

where n is the refractive index, λ is the wavelength and a , b and c are constants. The deviation in the red was thought to be due to an

absorption band in the infra red, but after all efforts to locate such a band had failed, Meggers and Peters concluded that equation (1) could satisfactorily be employed in representing the optical dispersion of air. Since 1918, spectroscopists have almost exclusively used tables based on the results of Meggers and Peters in converting air wavelengths to vacuum wave numbers.

During the period 1934-1939, Kosters and Lampe⁽⁴⁾, Perard⁽⁵⁾, and Barrell and Sears⁽⁶⁾ independently published dispersion formulae for visible radiations which are in fair mutual agreement, but which give values of refractive index appreciably higher than do the results of Meggers and Peters.

In 1950, Meggers and Kessler⁽⁷⁾ measured the wavelengths in air of 28 lines emitted by a $^{198}_{80}\text{Hg}$ source. In order to test their measurements by means of the combination principle, they reduced their air wavelengths to vacuum wave numbers with the aid of the dispersion equations of Meggers and Peters, and of Barrell and Sears. Recurring wave number differences indicated that the refractivity of air for ultra-violet relative to visible is too large as calculated from the formula of Meggers and Peters and too small when calculated from the formula of Barrell and Sears. It should be remembered, however, that Barrell and Sears' formula was based on observations in the visible spectrum and could not be expected to yield precisely the refractive indices for ultra-violet lines approaching the absorption band of air for short wavelengths.

To meet the demand of precision spectroscopists who require a dispersion formula more accurate than that of Meggers and Peters,

Edlén⁽⁸⁾ in 1953 combined dispersion relations of Koch⁽⁹⁾, range 4660 Å to 2378 Å, and of Traub⁽¹⁰⁾, range 5460 Å to 1854 Å, with that of Barrell and Sears, range 6438 to 4358, by choosing proportionality factors such that a 'best fit' of the two first-mentioned equations was obtained with the curve of Barrell and Sears. In this way he obtained 46 values of refractive index for 38 wavelengths ranging from 6438 Å to 1854 Å. The ordinary Cauchy relation was incapable of representing the data without systematic variations, and the following relation was found to be suitable:

$$n - 1 = a + \frac{b}{c - \sigma^2} + \frac{d}{e - \sigma^2} \quad (2)$$

where n is the refractive index, σ is the wave number and a , b , c , d and e are constants. Edlén estimates that his relation gives correct relative values of refractive index down to about 2000 Å with an accuracy of $\pm 1 \times 10^{-8}$, and that the errors in absolute values, depending directly on Barrell and Sears' data, should not be much greater.

During the present investigation, relative values of refractive index were determined for 18 wavelengths in the visible and ultra-violet spectral regions. A least squares procedure was then used in fitting the data first, to an ordinary Cauchy type relation with three constants and secondly, to an equation of the form:

$$n - 1 = A + \frac{B}{C - \frac{1}{\lambda^2}} \quad (3)$$

All measurements were made in dry, carbon dioxide-free air at about 21°C and 760 mm. of mercury pressure.

II THEORY

1. Theory of Refractive Index

The fundamental equation of classical dispersion theory is

$$n - 1 = \frac{4\pi N e^2}{m} \sum_l \frac{f_l}{\omega_{0l}^2 - \omega^2 + iK_l \omega} \quad (4)$$

where n is the complex index of refraction;

N , the number of molecules per unit volume in the dielectric medium each of which has f_l oscillators where

$$l = 1, 2, 3 \dots p;$$

f_l is the oscillator strength;

m, e , the electronic mass and charge, respectively;

$$\omega_{0l}^2 = \omega_{0l}^2 - \frac{4\pi}{3} \frac{N e^2}{m} f_l ;$$

ω_{0l} , the natural frequency of the oscillator; and

K , the absorption constant.

In regions of small absorption, $\omega_{0l}^2 - \omega^2 \gg iK_l \omega$; also, the imaginary part of the complex index may be neglected. For a wavelength region, then, removed from the absorption bands of air in the extreme ultra violet, we may write

$$n^2 - 1 \simeq 2(n-1) = \frac{4\pi N e^2}{m} \sum_l \frac{f_l}{\omega_{0l}^2 - \omega^2} \quad (5)$$

since $\omega_{0l}^2 \simeq \omega_{0l}^2$, N being much smaller in the case of air than for solids or liquids.

Equation (5) indicates that refractivity is proportional to density.

The right hand side may be expanded in the Cauchy form

$$n - 1 = a + b\lambda^{-2} + c\lambda^{-4} + d\lambda^{-6} + \dots \quad (6)$$

three terms of which are in general found to be satisfactory in representing the dispersion of air.

It would be expected that air, being a mixture, is not as suitable for the determination of precise physical laws as is a pure gas. Barrell and Sears have shown, however, that the refractivity of different samples of dry, carbon dioxide-free air is remarkably constant.

Considerable disagreement exists among various observers as to the exact dependence of the dispersion of air on temperature and pressure. Since refractive index is linked with the absorption of a substance, which in turn depends on temperature and pressure, it seems reasonable to assume that a slight variation in dispersion with temperature and pressure does exist. In view of this uncertainty, present measurements have been performed under conditions at which most interferometric work is done.

2. The Fabry Perot Interferometer.

The theory of the Fabry Perot interferometer has been discussed in detail by Meissner⁽¹¹⁾ and Tolansky⁽¹²⁾. Essentially, it consists of

two plane-parallel, partially-reflecting films separated a distance t (Fig.1). The path difference of two adjacent, coherent beams such

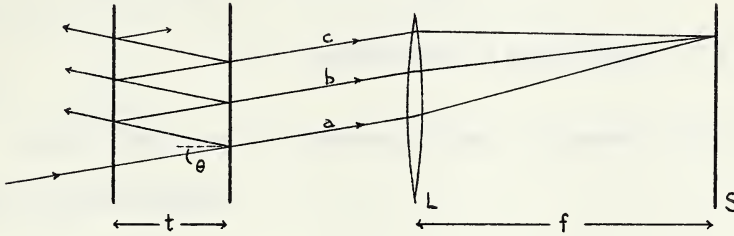


Fig. 1. Multiple Beam Transmitting Interferometer

as a and b , emerging from the interferometer is $2t \cos\theta$. If the number of wavelengths, λ , lying within this difference in path is P , then

$$P\lambda = 2t \cos\theta. \quad (7)$$

Constructive interference occurs at those values of θ for which P is an integer. The fringes, consisting of alternate bright and dark rings formed at infinity, are brought to a focus by a suitable lens.

The maxima are numbered $0, 1, 2, 3 \dots n$, starting from the centre, and defined by

$$p_n \lambda = 2t \left(1 - \frac{D_n^2}{8f^2} \right) \quad (8)$$

where p_n is the integral order number,

D_n , the diameter of the n^{th} maximum,

and f , the focal length of the lens.

Putting $i = n + 1$ and remembering that $p_n - p_1 = 1$, we obtain from (8)

$$D_i^2 - D_n^2 = \Delta D^2 = \frac{8f^2}{2t} \quad (9)$$

= a constant for a particular λ , f , and t .

At the centre of the pattern, since, in general, the order number P is not an integer,

$$\begin{aligned} (p_0 + e) &= 2t, \\ \text{or } (p_n + n + e) &= 2t. \end{aligned} \quad (10)$$

Inspection of equations (8) and (10) reveals that the partial order of interference,

$$e = \frac{D_n^2}{\Delta D^2} - n. \quad (11)$$

In determining e , it is desirable to average measurements on a number of diameters. A convenient method of doing this is provided by the method of least squares (Appendix C). The normal equations are:

$$je = \frac{1}{\Delta D^2} \sum D_n^2 - \sum n \quad (12)$$

$$e \sum n = \frac{1}{\Delta D^2} \sum n D_n^2 - \sum n^2 \quad (13)$$

where all summations are from $n = 0$ to $n = j - 1$, j being the number of fringes measured. In the case where $j = 5$,

$$e = \frac{3 \sum D_n^2 - \sum n D_n^2}{1/2 \sum n D_n^2 - \sum D_n^2} \quad (14)$$

Individual values of e may be calculated from

$$e_n = \frac{D_n^2}{\Delta D^2} - n \quad (15)$$

$$\text{where } \Delta D^2 = \frac{1}{5} \left(1/2 \sum n D_n^2 - \sum D_n^2 \right) \quad (16)$$

The standard deviation in e is

$$\left(\frac{\sum (e_n - e)^2}{5} \right)^{1/2} \quad (17)$$

The determination of exact etalon thickness, $2t$, is based on the first^{of} equations (10), namely,

$$(p_n + e)\lambda = 2t.$$

If at least two exactly known wavelengths (e.g. neon standards) are available and an approximate value of etalon thickness ($2t_x$) is known from measurements performed with a good screw micrometer, approximate order numbers ($p_{ox} + e_x$) may be obtained for each of the two standards from the ratios $2t_x/\lambda$. The order numbers are made precise in each case by using fractional parts determined from equation (14) and varying the integral portions by units until agreement of 2 or 3 parts in 10^8 is obtained in the products of exact wavelengths and corresponding order

number. A third standard wavelength is then used to check the value obtained for $2t$. Since neon standards are defined at 15°C and 760 mm. of mercury pressure, appropriate indices of refraction must first be used to convert them to exposure conditions.

3. Determination of Refractive Index of Air.

The determination of refractive index requires that interferograms of each employed radiation be obtained with the Fabry Perot interferometer in air and in vacuum. Two equations of the type (10) are then applicable:

$$\begin{aligned}(p + e)\lambda &= 2t \\ (p' + e')\lambda' &= 2t\end{aligned}\tag{18}$$

where the unprimed values refer to vacuum and the primed values refer to air.

Using (18) in conjunction with the definition of refractive index gives

$$n = \frac{\lambda}{\lambda'} = \frac{p' + e'}{p + e}\tag{19}$$

and

$$n - 1 = \frac{x + e' - e}{p + e}\tag{20}$$

where x has been substituted for $p' - p$. Since the order number is not required to high precision, we may use the first of equations (18) to obtain

$$n - 1 = \frac{\lambda(x + e' - e)}{2t} \quad (21)$$

Thus, to calculate refractivities we need to know:

- (a) the fractional parts for the wavelengths for which the refractive indices are desired;
- (b) the values of the wavelengths to six significant figures;
- (c) the thickness, $2t$, to six figures.

The integral order number difference, x , is determined in each case from an approximate value of $n-1$ in (21) obtained by means of equation (38), Appendix D, using an appropriate standard refractivity.

4. Phase Change on Reflection.

Upon reflection at metallic surfaces light penetrates the films a short distance giving rise to the phenomenon known as 'phase change on reflection'. As a result, the thickness of the etalon appears to change slightly with wavelength, the magnitude of the change being different for air and vacuum plates since corresponding wavelengths are slightly different.

Let $\delta(2t)$ be the apparent change in etalon thickness in vacuum, depending on the wavelength, λ , and $\delta'(2t)$ be the apparent change in air, depending on λ' . Proceeding as in section 3, we have

$$\begin{aligned}(p + e)\lambda &= 2t + \delta(2t) \\ (p' + e')\lambda' &= 2t + \delta'(2t)\end{aligned}\tag{22}$$

so that

$$n = \frac{\lambda}{\lambda'} \simeq \frac{p' + e'}{p + e} \left(1 + \frac{\delta(2t)}{2t} - \frac{\delta'(2t)}{2t} \right)$$

and

$$n - 1 = \frac{\lambda(x + e' - e)}{2t} + \frac{p' + e'}{p + e} \left(\frac{\delta(2t)}{2t} - \frac{\delta'(2t)}{2t} \right)\tag{23}$$

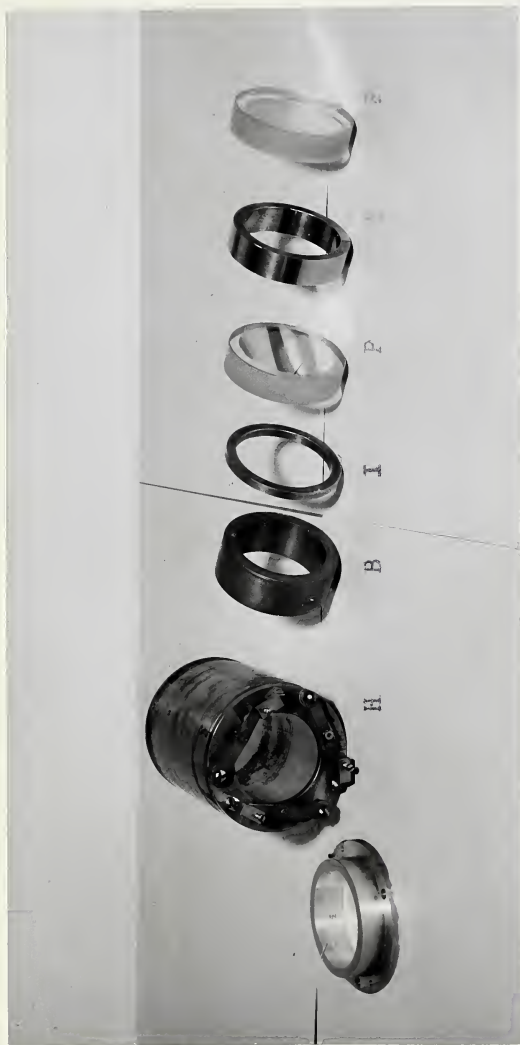
The phase change correction δ is small, usually in the eighth figure of $2t$, and since $\delta \simeq \delta'$, the difference $\delta - \delta'$ is even smaller. Because $2t$ is required only to 6 figures, the effect of phase change on reflection may be neglected.

III APPARATUS AND EXPERIMENTAL PROCEDURE.

1. Optical Apparatus.

The Fabry-Perot etalon (Plate I) used in the present determination of the dispersion of dry carbon dioxide-free air was of the variable gap type with invar ring spacers and quartz flats originally aluminized each on one side to a reflectivity of 80%. The details of its construction are dealt with elsewhere⁽¹³⁾. Although a number of tiny clear specks on the plates indicated that the aluminized surfaces might be blistering with age, the reflectivity had not yet gone down to a point where the quality of the interferograms was seriously affected.

Interferograms were taken with three different etalon spacings: 1.5 cm, 2.5 cm and 2.8 cm. Prior to the assembly of an etalon, the invar spacer was ground with rouge until the wedge angle subtended by the two quartz flats, under no external applied forces, was less than 2×10^{-5} radian. This was ascertained by viewing ring fringes with a relaxed eye positioned about a meter away from the etalon, on the opposite side of which was placed a mercury lamp, and noting a change in order number of less than two across the plates as the eye was moved along the direction of the wedge. To insure optical contact, the quartz flats were wrung into the invar spacer. Dark interference fringes could then be observed at the points



H Etalon Holder

B Brass Ring

I 'Invar' Ring

P Etalon Plates of

Crystal Quartz

S 'Invar' Spacer

PLATE I. AN UNASSEMBLED FABRY PEROT ETALON

of contact.

Care was taken during the final assembly of an etalon within its holder to align the projections on the spacer with the brass pins used in rendering the plates parallel. In this way, bending stresses in quartz flats were avoided.

Final adjustment of the plates for parallelism was done within the etalon chamber (see Fig. 2) at the temperature of the thermostatically controlled bath. It was discovered that an etalon rendered parallel at a temperature only three or four degrees different from operating temperature became disaligned at operating temperature. In setting the plates parallel, a low pressure mercury lamp was positioned in front of the quartz window at one end of the etalon chamber. At the other end of the chamber, from which the end plate had been removed, fringes of equal inclination were observed with a telescope with small aperture focussed for infinity⁽¹²⁾. The telescope was moved vertically and horizontally across the field of view and any change in the character of the central portion of the fringe system was observed. The test was especially sensitive if the central maximum or minimum was just at the point of appearing or disappearing. Tolansky estimates that in such an instance, a local variation in distance between the plates of one-fortieth of the employed wavelength can be detected.

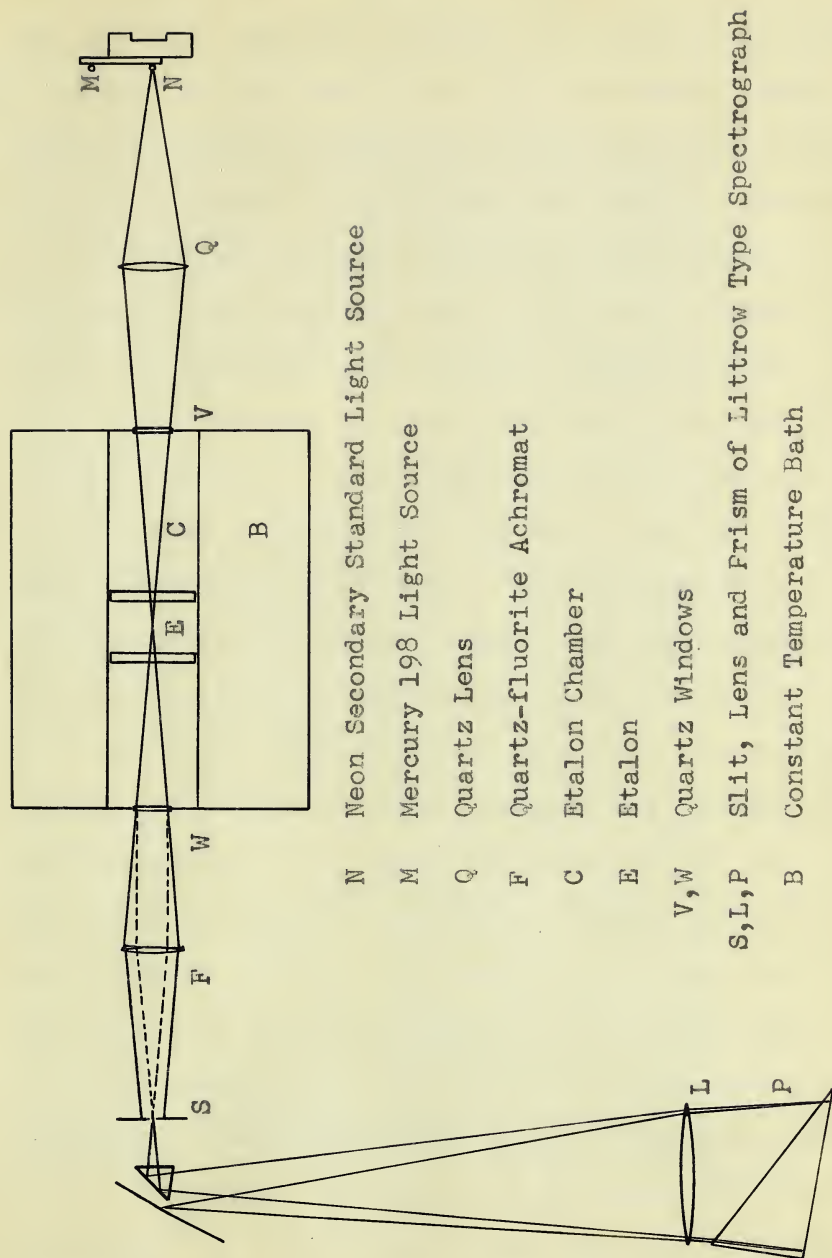
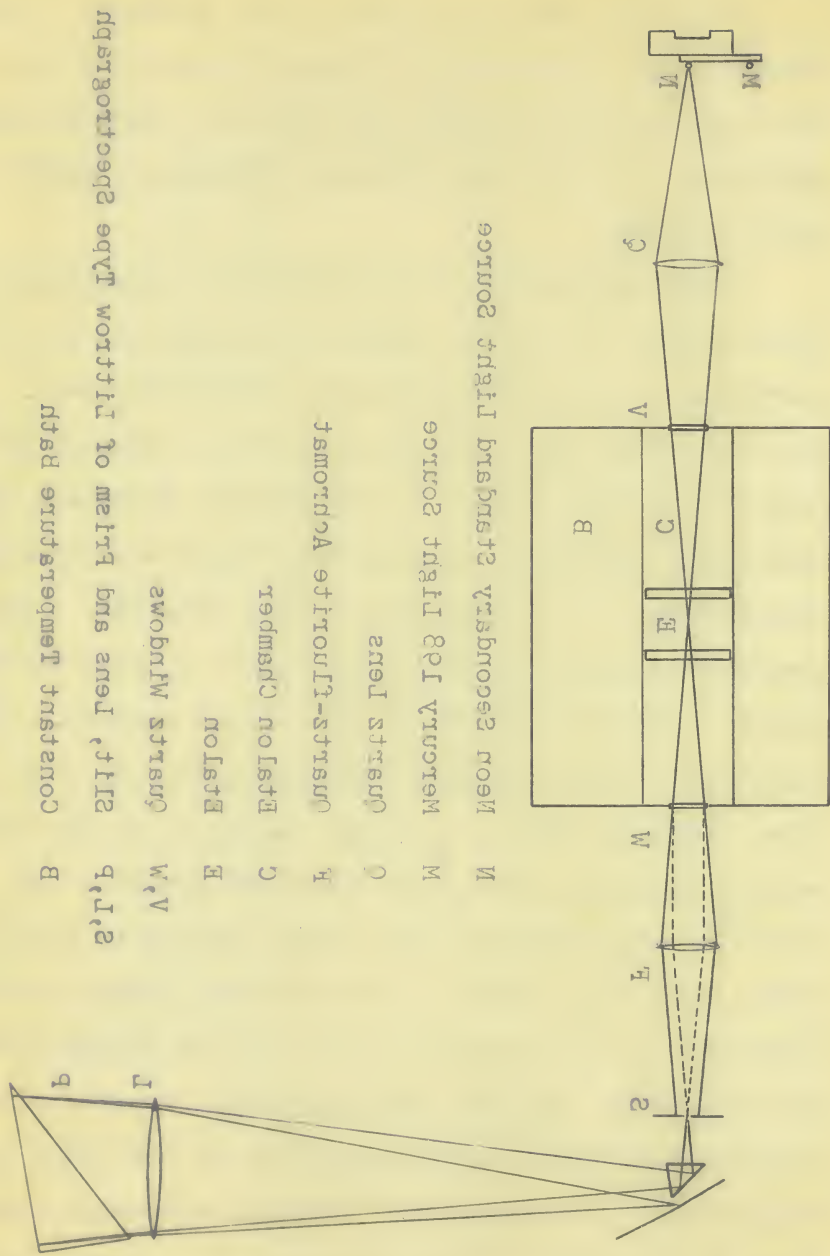


Figure 2. General Arrangement of Optical Apparatus

Figure 5. General Arrangement of Optical Apparatus



B Constant Temperature Bath

S, L, B Slit, Lens and Prism of Liffrow Type Spectrograph

V, W Quartz Windows

E Ersjon

C Ersjon Chamber

F Quartz-Fluorite Achromat

O Quartz Lens

M Mercury Tag Light Source

N Neon Secondary Standard Light Source

Etalons adjusted in the manner described above were found to be remarkably stable. The 2.8 cm. etalon, for example, remained parallel for a period of nearly a month. In the case of the 2.5 cm. etalon, whose spacer consisted of 1.0 cm. and 1.5 cm. invar rings placed together, the stability was somewhat decreased.

During the process of aligning the plates, it was discovered that one or both of them were slightly bowed. Since, in practice, only a small central portion of the plates is utilized, the observed defect was not considered to be serious. Also, weak secondary maxima and minima superimposed on the central maxima of the main Fabry-Perot pattern were detected. These belonged to a secondary fringe system formed between the aluminized and uncoated surfaces of the quartz flats which were cut at a slight wedge angle so as to displace the secondary fringe system to the side. Because the secondary maxima were relatively weak and positioned, at the centre of the main ring system, in a direction roughly parallel to the spectrograph slit, it was thought that they would in no way interfere with the quality of the final interferograms.

The particular method of positioning the etalon relative to the rest of the optical apparatus shown in figure 2 is known as the convergent beam method of mounting⁽¹²⁾. Light from either the neon secondary standard source, or the mercury - 198 source was focussed at a point approximately one-half-way between the interfero-

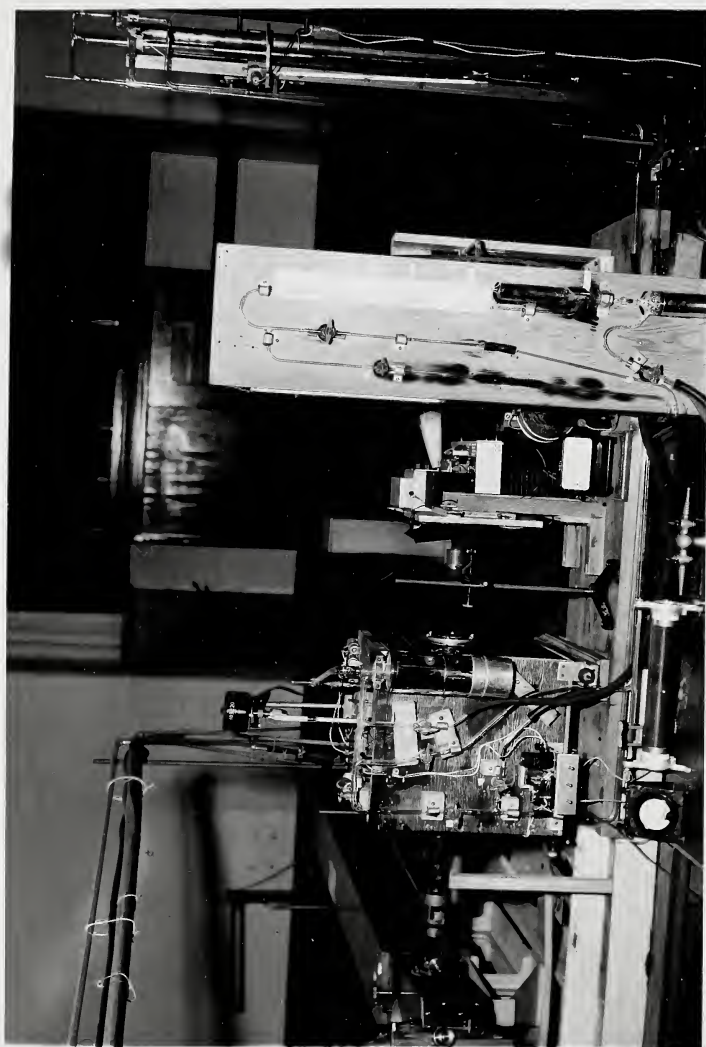


PLATE II. GENERAL VIEW OF THE APPARATUS

meter plates by means of the quartz lens, Q_1 . The light entered and left the etalon chamber, whose construction is adequately described by Smith⁽¹³⁾, through the quartz windows W_1 and W_2 . The interference fringes at infinity were then focussed on to the slit, S , of a Hilger E-1 Littrow type spectrograph with quartz optics (Appendix B) by the quartz-fluorite achromat Q_2 of focal length approximately 23 cm.

In centering the interference pattern on the slit of the spectrograph, an extended white light source was placed inside the spectrograph. An image of the slit was then reflected back by the etalon and appeared alongside the slit. Controls were provided for vertical and lateral motion of the insulated copper tank containing the water bath and etalon chamber. These were manipulated until the reflected slit image coincided with the slit, thereby, rendering the aluminized surfaces of the interferometer plates perpendicular to the optic axis of the apparatus.

2. Light Sources and Excitation.

The neon secondary standard light source was a capillary type Geissler tube activated by a direct current at high voltage supplied by the secondary of a transformer, the primary of which was connected to a variac. Full wave rectification was accomplished by a bridge type copper-oxide rectifier. A millimeter in the lamp circuit insured that the lamp was at all times

operated at one intensity.

The mercury-198 lamp obtained from Baird Associates, Cambridge, Massachusetts, was constructed of vycor glass and contained a few milligrams of artificially prepared $^{198}_{80}\text{Hg}$ and a trace of $^{199}_{80}\text{Hg}$. It was operated by a 600 megacycle per second war surplus radar transmitter which had two triode push-pull, tuned plate-tuned cathode oscillators working in parallel⁽¹⁴⁾.

3. Vacuum-Air System.

Exposures were taken in vacuum and also in air at a pressure of approximately 760mm. of mercury. The particular arrangement of tubing and stopcocks illustrated in Fig.3 enabled the following operations to be performed:

- (a) Isolation of the mercury manometer, B, from the rest of the system during vacuum exposure, at which time the residual chamber pressure was measured with a McLeod gauge, M;
- (b) Maintenance of a vacuum, during air exposures, on the vacuum side of the manometer, the quantity of the vacuum being again measured with the McLeod gauge.

The McLeod gauge used had been calibrated by Olafson.⁽¹⁵⁾

All vacuum tubing was constructed of glass. Continuous evacuation of either the etalon chamber or mercury manometer during exposures was accomplished by means of a mercury diffusion pump and also a mechanical vacuum pump placed on vibration mounts about five meters away from the main body of the apparatus so as to reduce the vibration level in the vicinity of the apparatus. Air

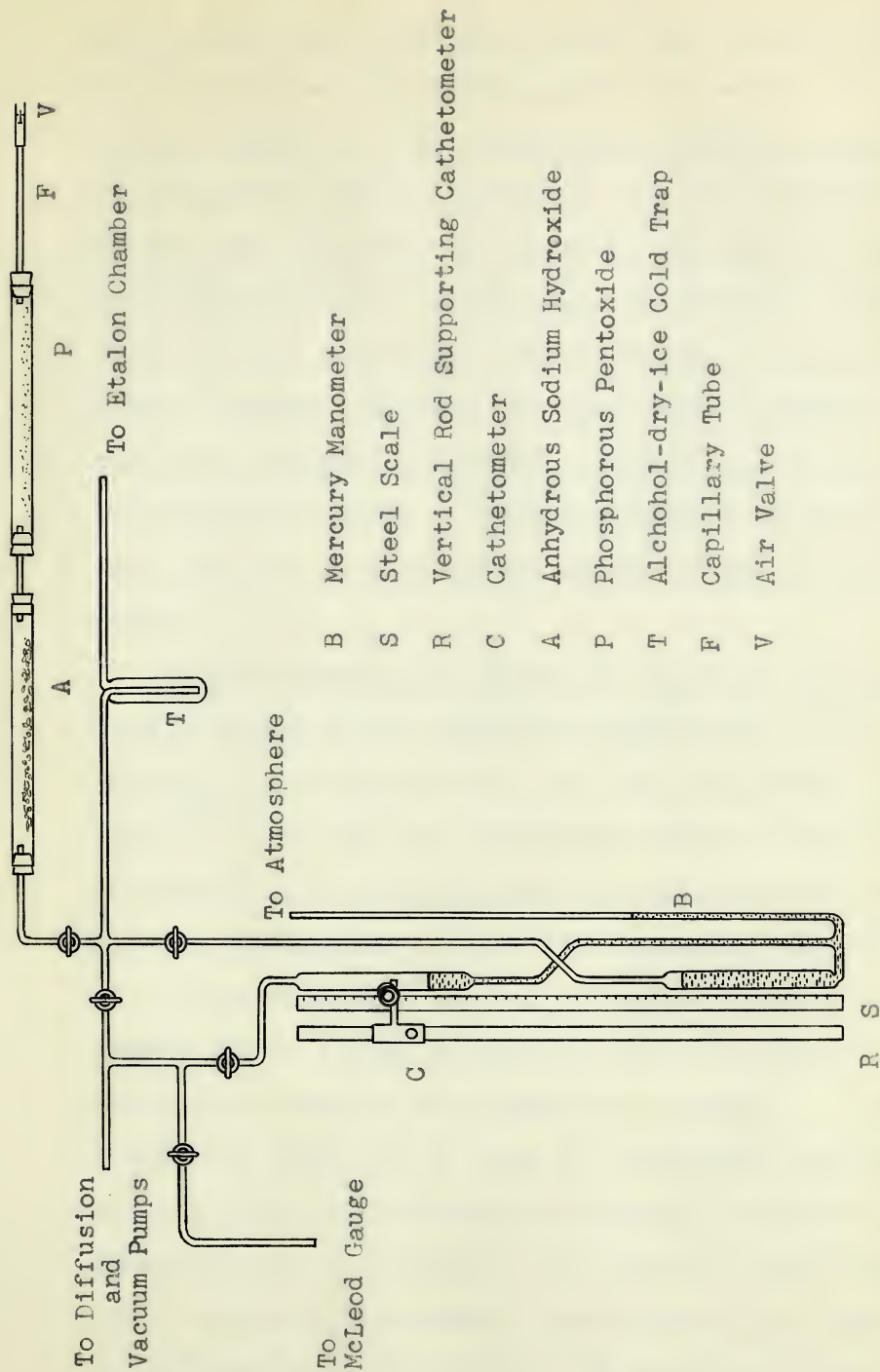
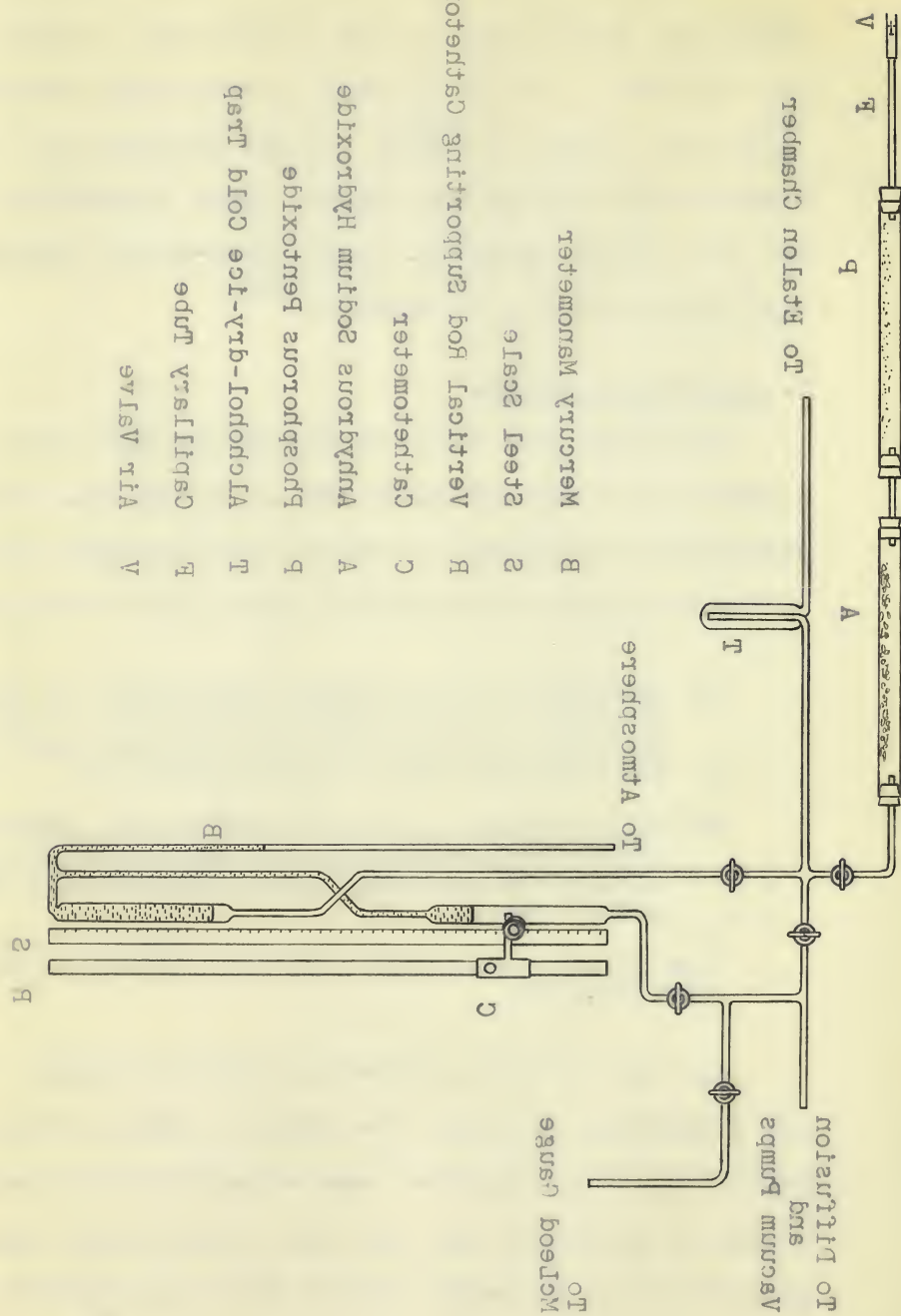


Figure 3. Schematic Diagram of Apparatus Used in Measuring Etalon Chamber Pressures

Figure 3. Schematic Diagram of Apparatus Used in Measuring Etalon Chamber Pressures



introduced into the etalon chamber was rendered free of water vapour and carbon dioxide by passing it through traps P and A, containing phosphorous pentoxide and anhydrous sodium hydroxide. The dry-ice-alcohol mixture in cold trap, T, served to prevent oil vapours from the mechanical vacuum pump, and mercury vapour from the diffusion pump, from diffusing back into the etalon chamber. Without the cold trap, resonance radiation occurred within the chamber, and it was impossible to obtain an interferogram of the mercury line 2536 A.V. even after an exposure time of several hours.

Chamber pressures during air exposures were measured by means of the barometer illustrated in Fig. 3. Details of its construction are fully discussed by Smith⁽¹³⁾. It has been mentioned earlier that it is necessary at the present stage in precision determination of wavelengths to know the refractive index of air to 9 significant figures at 10,000 Å, or the refractivity to 1 part in 30,000, since the value of refractive index is approximately 1.0003. Pressure, therefore, owing to the form of equation (38, Appendix D), must be known to 0.025 mm. in 760 mm. In practice, the cathetometer, C, mounted on the vertical supporting rod R, afforded a somewhat higher theoretical precision in the reading of pressures. The eyepiece of the low-power microscope contained a glass scale whose image was projected on to the steel scale, S, graduated in

millimeters, or, upon rotation of the cathetometer, on to the mercury column. Magnification was such that approximately 33 of the scale divisions in the eyepiece coincided with a single division on the steel rule. Estimates of the heights of the mercury columns were made to tenths of an eyepiece scale division, so that readings were made to 0.0033 millimeter of mercury. Actually the accuracy was considerably reduced due to non-uniformities of the rod about which the cathetometer was rotated. Discrepancies, too, of 0.01 millimeter was observed in steel scale millimeter divisions selected at random.

It is to be noted that in the present determination of relative dispersion, a knowledge of absolute pressure is unnecessary.

In general, the air pressure with the etalon chamber continuously increased during a sequence of exposures on one plate. This increase, which was caused by a drop in the level of the dry ice-alcohol mixture within the cold trap as the dry ice slowly evaporated, usually amounted to less than .5 mm. of mercury during a period of 3 hours.

The vacuum side of the mercury manometer was at all times maintained at a residual pressure of less than 2×10^{-5} mm. No correction to the pressure as observed on the manometer was, therefore, necessary. Neither were residual pressure corrections required in the case of vacuum exposures.

4. Constant Temperature Bath.

Constant temperature of the water bath which enveloped the etalon chamber was achieved by means of a continuous flow of water through a copper coil immersed in the bath, and a thermostatically controlled heater. Water flow and heater current were kept adjusted so that heating time very nearly equalled cooling time, the duration of a complete cycle being 4 minutes, which, incidentally, was the time of the shortest exposures on the plates. The water was stirred with a small propeller driven by an electric motor mounted on rubber shock-absorbers so as to minimize vibration. Variation in temperature of different portions of the bath, as indicated by a Beckmann thermometer (see Appendix A), was found to be less than 0.01 C. Temperature range during a cycle was slightly less than 0.02 C.

It is possible that some effect due to the variation in temperature during a cycle might exist. At 6000 Å the plate thickness, $2t$, must be known to an accuracy of 1.7 parts in 10^8 . The linear coefficient of expansion of 'invar' being $0.9 \times 10^{-6}/^\circ\text{C}$, a change in temperature of 0.02 C corresponds to a change in $2t$ (for a 1.5 cm. etalon) of 0.9 part in 10^8 . This figure lies well within the required precision. However, it has been pointed out⁽²⁾ that the overall temperature coefficient of the etalon may be considerably greater than that of the spacer. Since the steel etalon holder

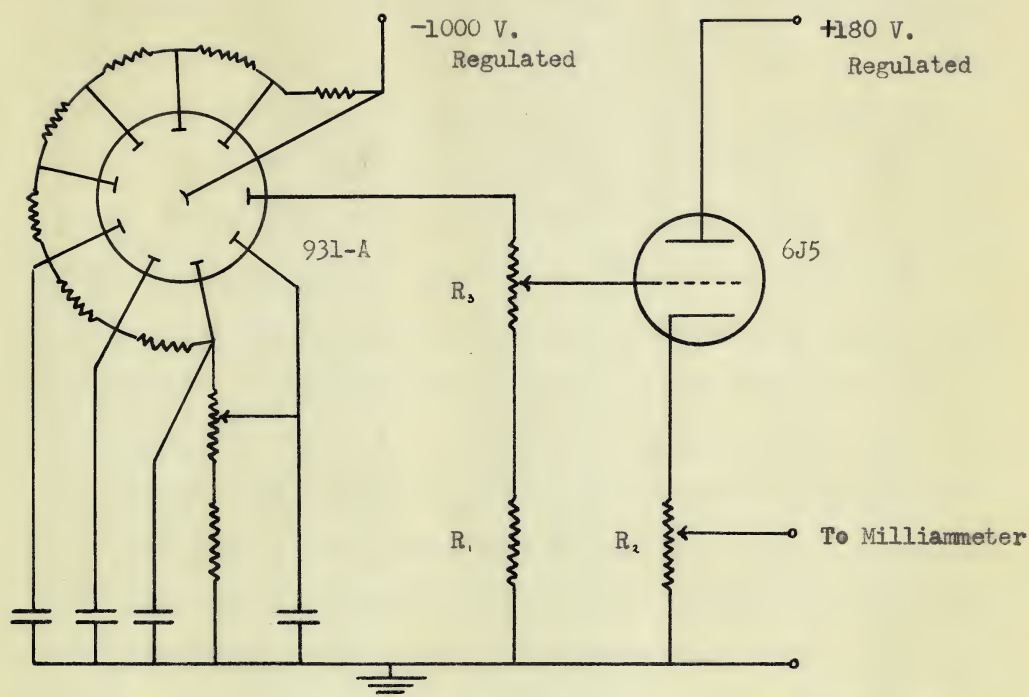


PLATE III. THE RECORDING DENSITOMETER

has a linear temperature coefficient approximately 12 times that of 'invar', the relative increase in the length of the holder with temperature is greater than that of the spacer. This results in a decrease in the tension on the springs holding the quartz flats against the spacer so that plate separation may increase.

5. The Densitometer.

A recording densitometer shown in Plate III and adequately described elsewhere^(13,15), used in analyzing the Fabry-Perot interferograms, was slightly modified in that the gear coupling between the screw of the densitometer and the Esterline Angus recorder was replaced by a direct drive linking the screw with the chart drive of the recorder. Distances on the photographic plate were directly translated on to the densitometer chart. In this way errors due to worn or dirty gears were avoided. The pitch of the densitometer screw was 1 mm. while the diameter of the chart drive drum was approximately 36 mm.; magnification was, therefore, about 114. Controls in the 931-A photomultiplier detector and cathode follower circuit shown in Fig.4 were manipulated so that the amplitude of the maxima on the charts was about 6 cm. Sharp peaks were in this manner avoided, and since the paper speed was slow (about 7.6 cm/minute), the lag in the milliammeter needle was not considered likely to result in an appreciable source of error.

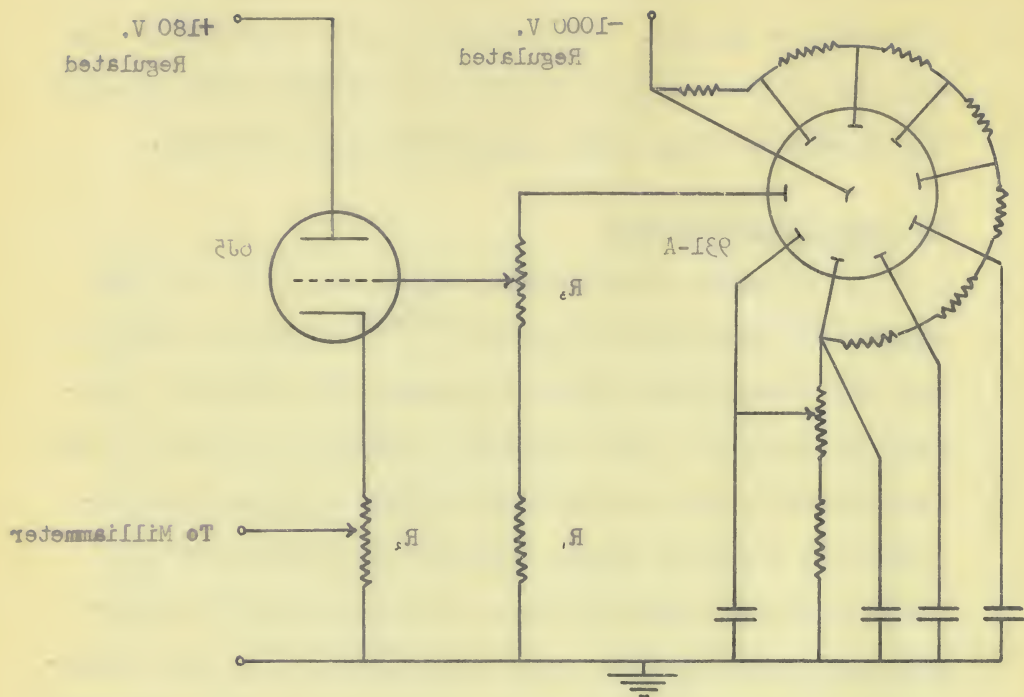


R_1 470,000 ohms
 R_2 10,000 ohms
 R_3 10 megohms
 Unmarked resistors 100,000 ohms each
 All condensers 0.01 mfd.

Figure 4. Photomultiplier Circuit.

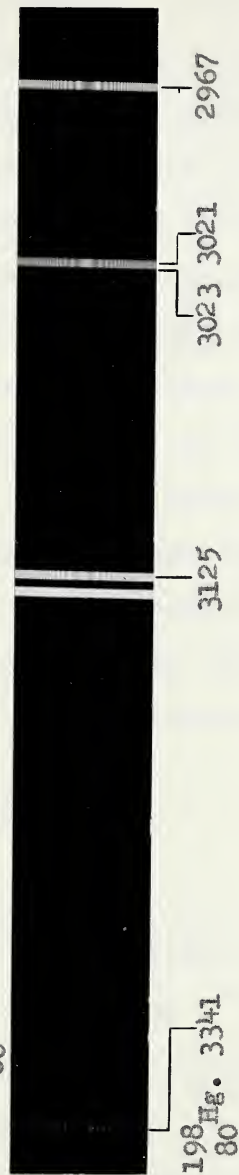
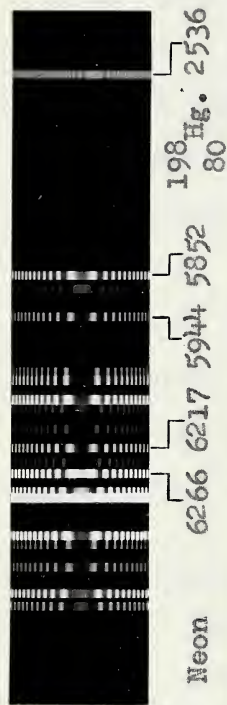
Figure 4. Photomultiplier Circuit.

R_1 470,000 ohms
 R_2 10,000 ohms
 R_3 10 megohms
 Unmarked resistors 100,000 ohms each
 All condensers 0.01 mfd.



Repeated tracings of a number of interferograms indicated the existence of random errors of about 0.002 millimeter in 1 millimeter. These may have been caused by non-uniformities in the densitometer screw, or by the bearings on which the screw was mounted. Although the pitch of a top quality screw should not vary by more than 0.001 millimeter in 1 millimeter⁽¹⁶⁾, the observed errors were not much greater than those introduced during the process of "picking" the maxima and measuring the pattern diameters; therefore, no correction was made for them. It should be pointed out that had tracings been made while the densitometer had not yet attained temperature equilibrium, or if care had not been exercised in aligning the interferograms properly with respect to the optical apparatus, the errors introduced would have been considerably greater. It was important, too, to have the optical system in good focus.

Ten innermost maxima on each interferogram were 'picked' by bisecting the outlines of the fringes. Measurements of the fringe diameters were then made to 0.01 inch with a good quality engineers' scale. During the 'picking' process it became apparent that the intensity distribution in many of the fringes, remote from the central maxima, was not symmetrical. A marked asymmetry occurred in an occasional fringe. It was thought that these irregularities may have been caused by minute departures from optical flatness of the interferometer



Etalon Thickness, $t = 2.8$ cm. Magnification: 2.6X

PLATE IV. SOME INTERFEROGRAMS FROM A TYPICAL PLATE

plates. In general, although the intensity distribution for an interferogram was very satisfactory in that the intensity decreased very gradually in the direction of the outermost fringes, the distribution within an individual fringe for many of the ultra-violet lines was only of fair. Tracings of these interferograms were somewhat jagged. Since precautions had been taken to avoid scratching the emulsion during the developing process, it is difficult to know what to attribute the observed effect to, except that perhaps the departures from optical flatness of the quartz plates were more pronounced for the shorter wavelengths. In the case of very weak lines where contrast was poor, it was necessary to increase the cathode follower gain considerably in order to obtain a measurable fringe on the recording paper. This resulted in some instability of the recording milliammeter.

6. Procedure in Taking Exposures.

i - Vacuum Exposures

The following sequences of timed exposures was taken on each of nine Eastman III - f plates, three plates being taken at each available etalon spacing:

- (a) Initial neon, 4 minutes;
- (b) Mercury - 2536 A.U., 4 minutes;
- (c) Mercury visible, $\frac{1}{2}$ hour;
- (d) Mercury ultra-violet, $1\frac{1}{2}$ hours;
- (e) Final neon, 4 minutes.

A separate exposure of the mercury - 2536 line was taken with spectrograph settings (see appendix B) such that the

line was focussed at the longer-wavelength end of the plate. In this way, better horizontal focus was achieved. Also, the 2536 line was badly over-exposed during the $1\frac{1}{2}$ hour ultra-violet exposure.

At least two hours before exposures were commenced, the constant temperature bath was placed in operation, and evacuation of the system was begun so that temperature equilibrium and constant residual etalon chamber pressure would be attained. The quality of the vacuum and the bath temperature were determined prior to and after each exposure.

ii - Air Exposures

Following the vacuum exposures on a plate, the etalon chamber was filled with dry, carbon dioxide-free air, after being flushed twice with such air, to a pressure of about 760 millimeters of mercury. At least one hour was allowed for the re-establishment of thermal equilibrium. The sequence of exposures given in (i) was then repeated. Bath temperature was determined before and after each exposure. Readings on the Beckmann thermometer were taken at 15 second intervals during a 4 minute cycle, and averaged. Pressures for the 4 minute exposures were determined once, while for the longer exposures, manometer readings were taken every 15 minutes, and averaged. Observed pressures were corrected for expansion of the steel scale; also, corrections were made for the temperature of the mercury and the gravitational acceleration. A total of nine air plates were taken, three with each

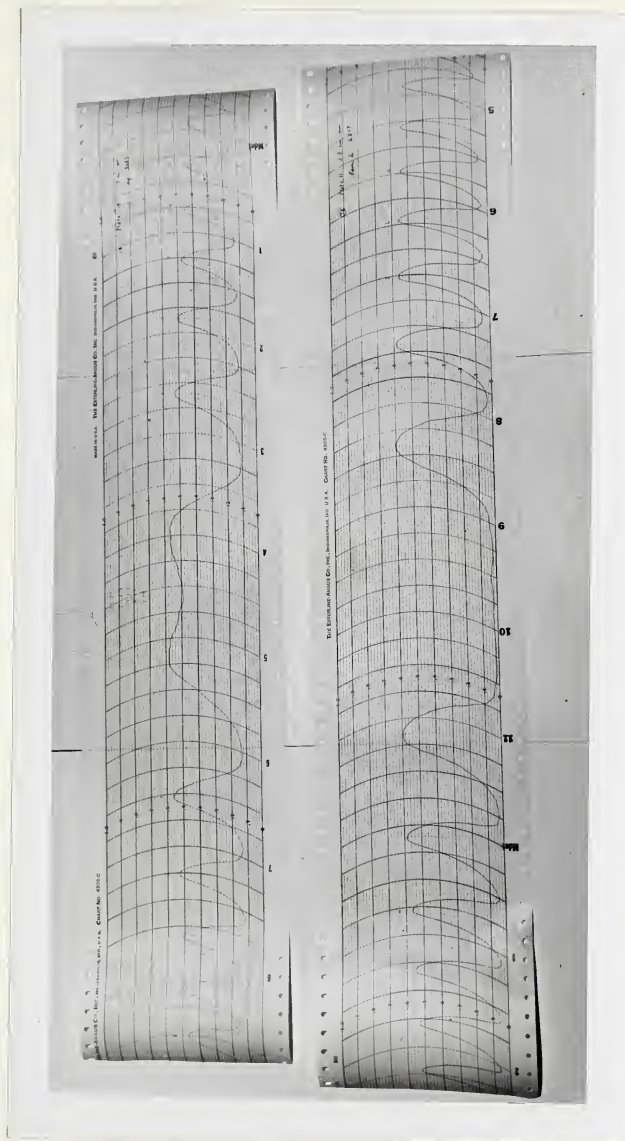


PLATE V. TYPICAL TRACINGS OF FABRY PEROT INTERFERENCE FRINGES

available etalon spacer.

The particular method of following up the vacuum exposure by the air exposures, described above, was adopted in order to study the effect of pressure on the etalon. The total exposure time for a 'vacuum' and an 'air' plate was about 8 hours, so that the 'drift' of the etalon springs was kept at a minimum value. Since the temperature of the etalon during this period was not altered significantly, it was thought that any difference that might be exhibited between values of plate thickness, 2 t, as determined from vacuum and air exposures, should be attributed to air pressure.

All plates were developed for 9 minutes in D-19 developer, fixed for 10 minutes in an acidfixer, and then washed in water for $\frac{1}{2}$ hour. While under water, the emulsion on a plate was rid of scum by brushing it lightly with a soft camel's hair brush. After washing, the plate was dipped for a few seconds in a wetting agent (Kodak Photo-Flo solution) and then dried in a cool stream of dust-free air within a specially built plate drier. Care was taken to insure that the developer, fixer, wash-water and wetting solution, were all at the same temperature. In spite of all the care taken in developing the plates, it was found that the emulsion on the Eastman III F plates had a tendency to peel.

IV EXPERIMENTAL DATA AND DISCUSSION

1. Effect of Air Pressure on the Etalon

The variation in etalon thickness with air pressure does not concern the present investigation of the dispersion of air; nevertheless, it is of considerable importance whenever absolute determinations of refractive index are made. Newbound⁽⁸⁾ has noted that the pressure coefficient of an etalon computed on the basis of compression of the spacer alone may be in error due to pressure effects on the etalon holder, springs, etc.

Results obtained at the present time are given in table I. In the second column are listed the fractional changes in lengths of the etalon spacers as computed from the relation

$$\frac{\delta(2t)}{2t} = \frac{\tau}{3} p \quad (24)$$

where τ is the volume compressibility of the spacer material and p is the air pressure. Actual values of $\delta(2t)/2t$ as determined from

TABLE I. Fractional Changes in Lengths of Spacers
due to Air Pressure.

<u>Etalon Thickness</u> <u>(2t)</u>	$\frac{\delta(2t)}{2t}$ (computed)	$\frac{\delta(2t)}{2t}$ (observed)
3.0 cm.	0.28×10^{-6}	0.33×10^{-6}
5.0 cm.	0.28×10^{-6}	0.20×10^{-6}
5.6 cm.	0.28×10^{-6}	0.04×10^{-6}

measurements on eight sets of air and vacuum plates are given in the third column.

The etalon utilized consisted of an 8.5 cm. long steel holder containing the quartz flats, an invar spacer and a brass 'filler' ring. An examination of the linear compressibilities of the materials indicates that the relative decrease with pressure in the length of

TABLE II. Elastic Constants of Materials

Material	Linear Compressibility $\tau/3 \times 10^{12}$ cm. ² /dyne
Crystal quartz	1.23
Brass	0.37
Invar	0.28
Steel	0.18

the internal components of the etalon should be greater than that of the holder. This should have the effect of releasing the tension on the springs and increasing plate separation. The expected result seems to have occurred in the case of the 2.8 cm. etalon (see Table I); for the remaining two spacings, however, the decrease in plate separation is fairly well predicted from considerations of compression of the spacers alone.

In view of the present findings it seems likely that the amount of tension on the etalon springs may be the controlling factor in change of plate separation with air pressure. Pressure corrections, therefore, based on constants of the materials alone, may not be always reliable.

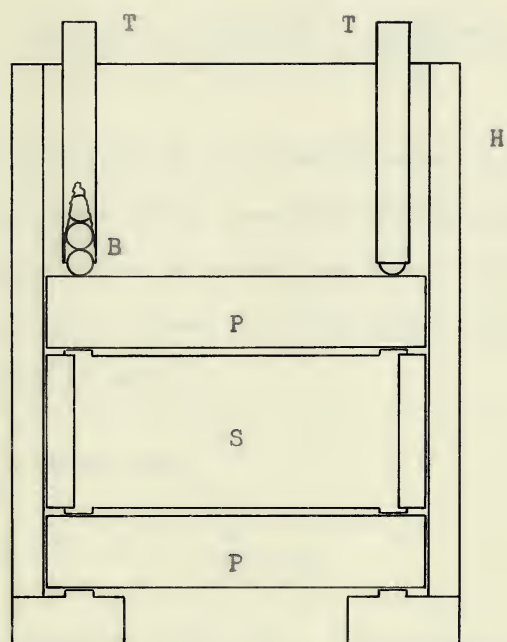
It seems possible that an etalon can be devised for which the pressure and temperature coefficients may be determined fairly accurately. Such an etalon is shown in figure 5. Unlike common interferometers, it would be employed with its optic axis positioned vertically. Adjusting springs would be eliminated; instead, steel balls within polished guide tubes could be used in rendering the plates parallel. It is felt that such an etalon could be maintained in adjustment for an indefinite period of time since the downward forces exerted by the steel balls would never vary significantly. With proper alignment the friction between the steel balls and polished guide tubes could be practically eliminated so that changes in the dimensions of the etalon holder with pressure or temperature would have no effect on the etalon proper. If the friction forces are appreciable, parallelism of the etalon may be achieved by simply placing small weights near the edge and on top of the upper plate.

2. Dispersion Curves For Air

The mean values of refractivity (see table IX, Appendix E) determined from measurement on 18 wavelengths in the spectral range 2536 Å to 6266 Å, were fitted to a Cauchy type relation by the method of least squares. The resulting relative dispersion equation is

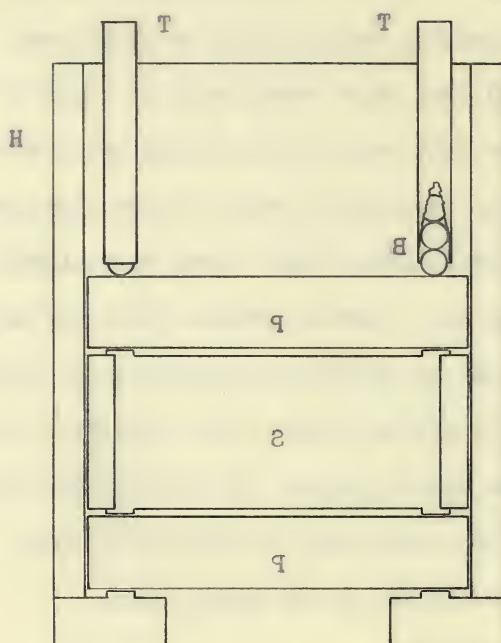
$$(n - 1) \times 10^6 = 272.648 + \frac{1.462\ 483}{\lambda^2} + \frac{0.020\ 641}{\lambda^4} \quad (25)$$

(λ is the vacuum wavelength in microns).



- | | | | |
|---|-----------------------------|---|---------------|
| P | Etalon Plates | H | Etalon Holder |
| S | Spacer | B | Steel Balls |
| T | Guide Tubes Fixed To Holder | | |

Figure 5. Cross-section of a Vertical Type Etalon



P Etalon Plates
 S Spacer
 B Steel Balls
 T Guide Tubes Fixed To Holder
 H Etalon Holder

Figure 5. Cross-section of a Vertical Type Etalon

After adjusting to obtain a 'best fit' with averaged data of Barrell and Sears, and of Perard, in the visible spectral range, and correcting to standard air containing 0.03% carbon dioxide, equation (25) becomes

$$(n - 1) \times 10^6 = 272.773 + \frac{1.462\ 720}{\lambda^2} + \frac{0.020\ 644}{\lambda^4} \pm 0.044 \quad (26)$$

where the error indicated is the standard error of estimate. A comparison of values of refractive index (see table III) calculated by means of (26) with averaged values of Barrell and Sears, and of Perard, indicates a discrepancy of about 3 parts in 10^8 at 7000 Å and 4 parts in 10^8 in the opposite direction at 4000 Å.

An equation of the form

$$(n - 1) = A + \frac{B}{C - 1/\lambda^2} \quad (27)$$

was also fitted to the observed data. The constant, C, was determined by substituting into (27) the following three observed values of refractivity and corresponding wavelengths:

λ	$(n-1) \times 10^6$
6268.23	276.460
4047.71	282.377
2537.21	300.367

Constants A and B were then obtained from a least squares solution.

The resulting relative curve is defined by

$$(n - 1) \times 10^6 = 114.440 + \frac{16400.77}{103.7661 - 1/\lambda^2} \quad (28)$$

which becomes, upon adjustment to standard air,

$$(n - 1) \times 10^6 = 114.551 + \frac{16403.43}{103.7661 - 1/\lambda^2} \pm 0.041 \quad (29)$$

(λ is the vacuum wavelength in microns).

Values of refractive index determined from (29) are in much better agreement with averaged data of Barrell and Sears, and of Pérard, than are those calculated by means of equation (26).

For purposes of comparison, results of Meggers and Peters, and Edlén are also listed in table III. It has been mentioned previously that Edlén determined his dispersion equation by combining data obtained by Barrell and Sears from measurements made in the visible spectral region, with that of Koch, and Traub who worked with ultra violet wavelengths. Edlén estimates that his dispersion equation gives relative values of refractive index correct to 1 part in 10^8 . Meggers and Peters' values are then too small in the visible down to about 2500 Å, and too large below 2500 Å. On the other hand, values determined by means of equation (29) are in excellent agreement with those of Edlén down to about 3000 Å. At 2750 Å, equations (26) and (29) give indices greater

TABLE III. $(n - 1) \times 10^6$ for Standard Air.

Wavelength A	(a) Barrell and Sears	(b) Perard	Average of (a) and (b)	Meggers and Peters	Edlen	Equation (26)	Equation (29)
7000	275.789	275.845	275.817	275.301	275.790	275.844	275.803
6000	276.972	276.984	276.979	276.333	276.971	276.995	276.980
5000	278.967	278.945	278.956	278.131	278.964	278.954	278.970
4000	282.738	282.789	282.764	281.718	282.755	282.721	282.764
3000				290.692	291.557	291.574	291.589
2500				301.420	301.452	301.457	301.450
2000				325.631	324.076	322.244	322.806

by 2 parts in 10^7 , while at 2000 Å the deviation is about 6 times as large and in the opposite direction.

Formula (29) was tested by applying the combination principle to wavelengths of the $^{198}_{80}\text{Hg}$. spectrum determined by Meggers and Kessler⁽⁷⁾. The results are tabulated below.

TABLE IV. Recurring Intervals in the Spectrum of $^{198}_{80}\text{Hg}$.

Pair of Wavelengths	Interval in cm^{-1}	
	using equation (29)	using Edlén's equation *
4046 — 4358	1767.2176	1767.2183
2967 — 3131.5	.2160	.2173
2752 — 2893	.2192	.2190
4358 — 5460	4630.6766	4630.6765
3131.8— 3663.2	.6774	.6785
3131.5— 3662.8	.6771	.6779
3125 — 3654	.6777	.6777
2893 — 3341	.6782	.6791
2655 — 3027	.6812	.6812
3663.2— 5790	10025.7676	10025.7678
3654 — 5769	.7670	.7677
3027 — 4347	.7678	.7687

* Results obtained by Edlén⁽⁷⁾.

Inspection of the table reveals that the use of either equation (29) or Edlén's equation results in intervals which are comparably constant. It should be noted that the constancy of the intervals depends on an accurate knowledge of exact wavelengths.

Observed mean values of refractivity reduced to standard conditions and compared with corresponding calculated values indicated that the observed index for the wavelength 2752 Å was probably too large as compared to the rest of the values. The interferogram of the line 2752 Å was of very low intensity and it was found that refractive indices determined from measurements on very weak lines were characteristically higher. For that reason, indices originally determined for the weak lines 5790 Å and 4704 Å were not used in the present calculations. The possibility must be considered, however, that in more heavily exposed lines an overall shrinkage of the interference patterns occurred due to the fact that the blackened parts dried out more rapidly than the neighboring unexposed emulsion on the plates. In general, it was found, too, that fringes in the ultra violet were less sharp than were those in the visible. This was probably due to a decrease in the reflectivity of aluminum at short wavelengths.

APPENDIX A

Calibration of the Beckmann Thermometer

In calibrating the Beckmann thermometer on an absolute scale, bulb (G) of the apparatus shown in figure 6 was surrounded by a solid-carbon - dioxide - alchohol mixture and water was distilled into it from trap (E) by evacuating the manometer with stopcocks (B), (C) and (D) open. Stopcock (B) was then closed, and in a similar manner, the water in bulb (G) was redistilled into bulb (H). The cold trap, (F), served to prevent any moisture from reaching the vacuum pumps. Stopcock (C) was now closed and the residual pressure in the system reduced to less than 0.01 mm. of mercury. Water vapour present was, therefore, frozen out in bulbs (H) and (F). Stopcock (D) was finally closed and while a high quality vacuum was maintained in the right-hand column of the U-tube, (J), bulb (H) was inserted into a thermos bottle containing water and the Beckmann thermometer. As the ice in bulb (H) melted, the water vapour depressed the left-hand mercury column in the U-tube. After temperature equilibrium had been attained, ten measurements of the difference in heights of the two mercury columns, (J), were made by means of a travelling microscope fitted with a light source and a collimating lens. These measurements were averaged and corrected for difference in heights of the columns at zero pressure, and for the temperature of the mercury and the acceleration due to gravity. Measurements were repeated at five different temperatures of the water bath.

Vapour pressures were converted to temperatures with the aid of a table in the Handbook of Chemistry and Physics¹⁶⁾. These, together with

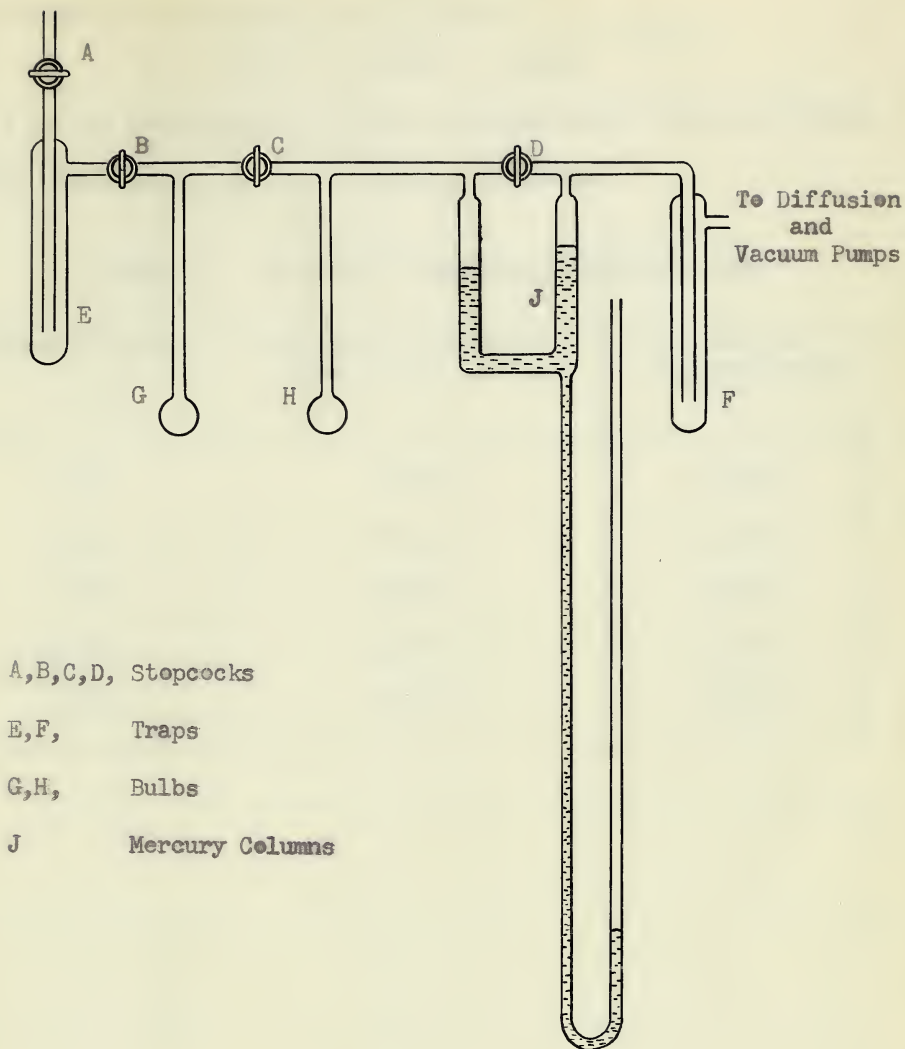
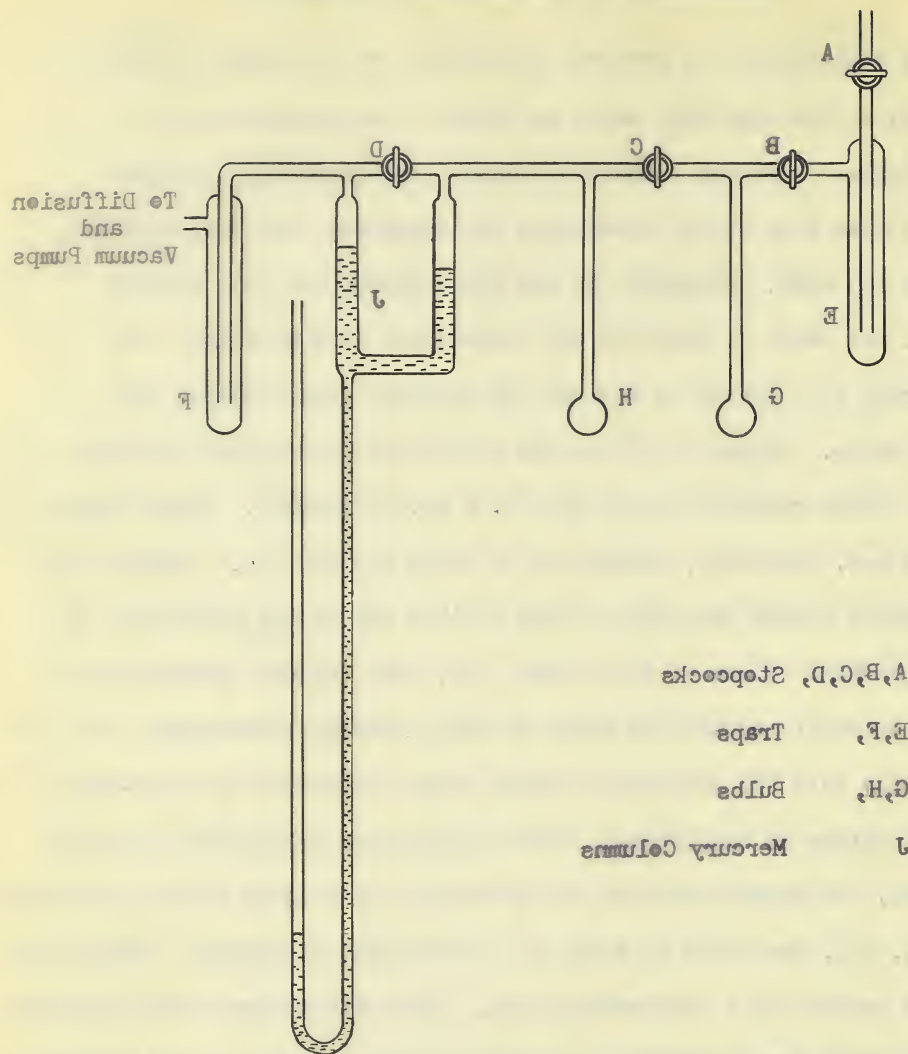


Figure 6. Manometer Used in Calibrating the Beckmann Thermometer

Figure 6. Manometer Used in Calibrating the Beckmann Thermometer



the mean readings of the Beckmann thermometer were used in deducing by the method of least squares the relation

$$T = 17.054 + 1.015B \pm 0.006$$

where T is the temperature in degrees Centigrade and B is the Beckmann reading. The standard error of estimate is given.

TABLE V Beckmann Thermometer Calibration Data

Beckmann Reading B	Corrected Difference in Height in mm. of Hg.	Temperature in Deg. Centigrade T
2.553	17.152	19.644
2.815	17.446	19.918
3.369	18.054	20.472
3.826	18.570	20.930
4.297	19.140	21.423

... ..

... ..

... ..

... ..

... ..

... ..

...
...
...
...
...
...

... ..

APPENDIX B.

Horizontal Focus of the Spectrograph

In crossing the Fabry Perot interferometer with a spectrograph it is important that the fringes be properly focussed on the spectrograph plate. Since the vertical-slit focus is slightly concave for a Hilger E-1 spectrograph, whereas the horizontal-fringe focus is convex, it was necessary to determine the best average focus. This was accomplished by examining images on spectrograph plates of fine glass threads stretched across the slit. It was found impossible to obtain satisfactory focus for lines distributed over the entire length of a 10 inch plate. For this reason, the spectrum to be photographed was divided into three portions and focussed in a manner such that the fringes fell on the 'longer-wavelength end' of the plate placed in an average focus. The horizontal focus settings determined are given in the table below.

TABLE VI. Horizontal Focus Settings of Hilger E-1 Spectrograph

Wavelength Range	Prism Rotation	Focus	Plate Tilt
7000A - 3400A	18.03	15 - 15	5.5
3400A - 2600A	14.83	37 - 6	13.3
2600A - 2400A	12.0	24 - 17	16.0

APPENDIX C.

Method of Least Squares.

The method of least squares enables a general equation of the form

$$Y = C_1 + C_2X + C_3X^2 + \dots \quad (31)$$

to be fitted to a number of data in such a way that the sum of the squares of the differences between the final curve and actual values is a minimum. If the given data is designated by the k points (X_i, Y_i) , then the least squares principle requires that the quantities

$$\frac{\partial \sum_i (Y_i - Y)^2}{\partial C_j} = 0 \quad (32)$$

where Y is the computed value. Equations (32) are known as the "normal" equations. They may be solved for the constants C_1, C_2, C_3, \dots etc.

The normal equations may also be obtained by multiplying the type equation (31) through in turn by the coefficient of each unknown and summing over all points. The resulting equations are

$$\begin{aligned} \sum_i Y_i &= C_1 k + C_2 \sum_i X_i + C_3 \sum_i X_i^2 + \dots \\ \sum_i X_i Y_i &= C_1 \sum_i X_i + C_2 \sum_i X_i^2 + C_3 \sum_i X_i^3 + \dots \\ \sum_i X_i^2 Y_i &= C_1 \sum_i X_i^2 + C_2 \sum_i X_i^3 + C_3 \sum_i X_i^4 + \dots \\ &\dots \quad \dots \quad \dots \quad \dots \quad \dots \end{aligned}$$

The standard error of estimate in the final equation is given by

$$\sqrt{\frac{\sum_i (Y_i - Y)^2}{k}}$$

APPENDIX D.

Reduction of Relative Dispersion Equations to Standard Conditions, and of Neon Standards to Exposure Conditions.

The relative curves derived from the observed data were adjusted to normal conditions of temperature and pressure (150°C and 760 mm. of mercury) by obtaining a 'best fit' with averaged values of refractive index determined from the formulae of Barrell and Sears, and of Perard. These formulae are:

$$(n - 1) \times 10^6 = 272.585 + 1.5437\lambda^{-2} + 1.293\lambda^{-4} \quad (33)$$

Perard

$$(n - 1) \times 10^6 = 272.860 + 1.4014\lambda^{-2} + 2.998\lambda^{-4} \quad (34)$$

(λ = vacuum wavelength in microns).

Relations (33) and (34) are applicable to standard air containing 0.03% carbon dioxide. They were, therefore, reduced first to normal air by means of the equation

$$\begin{aligned} (n - 1)_{\text{standard air}} &= 1 + 0.003 \frac{n_{\text{CO}_2} - n_{\text{air}}}{(n - 1)_{\text{air}}} (n - 1)_{\text{CO}_2 - \text{free air}} \\ &\approx 1.000162 (n - 1)_{\text{CO}_2 - \text{free air}}. \end{aligned} \quad (35)$$

The following data were then obtained:

λ	$(n - 1) \times 10^6$
4000	282.718
5000	278.911
6000	276.934
7000	275.722

Equation (35) was finally used to adjust the experimental curves to standard air.

In calculating the etalon spacing, $2t$, for the air exposure, it was necessary to reduce the neon secondary standards to exposure conditions. For the purpose, the relation

$$\frac{n-1}{\rho} = \text{constant} \quad (36)$$

and the ideal gas law

$$\frac{\rho_1 T_1}{P_1} = \text{constant} \quad (37)$$

were combined to give

$$(n_1 - 1) = \frac{P_1 T_2}{P_2 T_1} (n_2 - 1) \quad (38)$$

where n_1 and n_2 are the refractive indices at pressure, temperatures and densities P_1 , T_1 , ρ_1 , and P_2 , T_2 , ρ_2 , respectively. The neon secondary standards were first reduced to vacuum wavelengths with the aid of appropriate standard indices of refraction. Values of refractive index calculated from equation (38) were then used to obtain the vacuum standards at etalon conditions.

APPENDIX E

Observed Data

TABLE VII. Partial Orders of Interference for Vacuum Exposures*

Wavelengths	Plates (2t = 2.999 924 cm.)			Plates (2t = 5.000 170 cm.)**			Plates (2t = 5.598 544 cm.)		
	1	2	3	4	5	6	7	8	9
Initial No. 5852	.7506 ±30	.7576 ±20	.7559 ±31	.0225 ±36	.9863 ±30	.9876 ±25	.4099 ±35	.4237 ±27	.4189 ±34
5944	.7311 ±25	.7375 38	.7325 32	.2336 16	.1997 13	.2156 38	.8565 25	.8670 37	.8604 34
6217	.0336 ±35	.0373 09	.0305 22	.5293 11	.4972 38	.5001 18	.2035 20	.2058 26	.2115 10
6266	.2031 ±37	.2033 36	.2020 22	.1038 33	.0703 22	.0781 40	.2154 17	.2085 19	.2214 26
Final No.									
5852	.7573 ±34	.7616 16	.7566 03	.0157 16	.9901 30	.9895 27	.4192 30	.4206 24	.4151 22
5944	.7346 ±09	.7345 25	.7354 36	.2292 29	.2063 21	.2085 14	.8513 25	.8638 36	.8617 25
6217	.0328 ±26	.0371 10	.0318 25	.5220 26	.4979 24	.4978 27	.2061 20	.2088 33	.2114 28
6266	.1985 ±20	.2002 36	.1991 20	.1016 24	.0752 25	.0749 04	.2088 26	.2118 26	.2158 28
¹⁹⁸ Hg. 80									
2536	.3938 ±48	.3838 46	.3865 52	.0756 30	.9970 25	.0028 44	.4112 52	.4146 75	.4479 16
2652	.7818 ±29	.7913 40	.7812 39	.2127 52	.1635 140	.1977 67	.2248 72	.2223 59	.2023 70
2752	.6340 ±40	.6563 60	.6220 39	.9011 60	-	.8367 128	.4531 22	.4827 41	.5013 13
2893	.1445 ±35	.1457 46	.1354 23	.5214 56	.4531 67	.4909 50	.6542 62	.6600 75	.6620 74
2967	.5222 ±32	.5272 22	.5143 33	.9078 55	.8420 74	.8624 60	.6961 71	.6875 30	.7001 58
3021	.0236 ±55	.0306 29	.0202 50	.2364 36	.1668 37	.1869 27	.2942 58	.3051 53	.2998 30
3125	.2061 ±17	.2103 35	.1976 66	.8698 42	.7971 67	.8125 51	.1502 69	.1396 59	.1652 32
3341	.4675 ±19	.4682 25	.4692 41	.3355 53	.2861 50	.3033 40	.6048 29	.6221 36	.6135 21
3650	.7874 ±51	.7886 19	.7719 53	.1287 31	.0738 31	.0991 18	.5331 75	.5219 53	.5202 26
3663	.4276 ±18	.4261 13	.4278 42	.5008 15	.4435 28	.4609 32	.1864 52	.1997 56	.2100 12
4046	.0328 ±41	.0367 26	.0239 24	.7440 44	.6954 17	.7081 33	.7049 32	.7184 42	.7236 50
4077	.7790 ±58	.7895 31	.7724 55	.5970 45	-	.5694 03	.2242 31	.2257 56	.2316 20
4358	.5049 ±19	.5143 26	.4982 24	.3448 20	.3043 45	.3171 24	.8720 29	.8733 13	.8796 14
5460	.8164 ±27	.8254 10	.8226 30	.1650 16	.1295 10	.1399 25	.7975 37	.8127 40	-

* Values determined by A.A. Schultze⁽²⁰⁾

** Except Plate 4, 2t = 5.000 172 cm.

Standard deviations indicated are in the last two figures of the fractions.

TABLE VIII. Partial Orders of Interference for Air Exposures

Wavelengths	Plates (2t = 2.999 923 cm.)				Plates (2t = 5.000 169 cm.)*				Plates (2t = 5.598 544 cm.)			
	11	12	13	14	15	16	17	18	19	20	21	22
Initial Ne.												
5852	.6015 ±22	.5686 ±18	.5492 ±09	.2397 ±33	.1452 ±22	.0249 ±27	.2922 ±09	.2981 ±40	.2981 ±22			
5944	.3563 19	.3211 03	.2984 09	.0854 18	.9784 18	.8671 24	.3045 40	.3153 44	.3163 19			
6217	.0451 24	.0167 12	.9923 18	.3485 15	.2544 19	.1464 15	.5140 30	.5192 37	.5204 19			
6266	.1089 27	.0789 12	.0599 18	.7456 36	.6492 12	.5367 24	.3138 42	.3207 27	.3259 25			
Final Ne.												
5852	.6077 07	.5749 18	.5535 25	.2518 34	.1700 24	.0539 24	.3098 43	.3184 25	.3161 33			
5944	.3654 09	.3287 10	.3048 22	.0927 13	.0015 25	.8835 19	.3257 24	.3359 33	.3264 12			
6217	.0544 33	.0203 18	.0000 15	.3641 16	.2720 18	.1594 22	.5295 47	.5335 25	.5321 18			
6266	.1154 07	.0840 07	.0624 15	.7579 39	.6640 22	.5530 25	.3300 15	.3337 42	.3362 18			
¹⁹⁸ Hg. 80												
2536	.0341 30	.9388 27	.8792 22	.1551 70	.9387 27	.6439 47	.1205 71	.1508 56	.1371 28			
2652	.6296 47	.5189 37	.4892 56	.2583 36	.0434 105	.7842 77	.5152 98	.5655 73	.5517 44			
2752	.0554 22	.9897 21	.9282 47	-	-	.0942 56	.1383 73	.1945 74	.1670 50			
2893	.7695 24	.6998 37	.6420 33	.2182 65	.9940 73	.7716 37	.0155 10	.0342 92	.0058 56			
2967	.3102 27	.2280 25	.1871 33	.1776 56	.9820 15	.7487 03	.4376 56	.4649 36	.4561 56			
3021	.2219 22	.1526 27	.0992 71	.5145 50	.3249 27	.0917 37	.9336 30	.9719 43	.9505 28			
3125	.3319 25	.2616 37	.2158 53	.3473 55	.1784 71	.9512 30	.8091 47	.8272 16	.8023 50			
3341	.6327 19	.5715 19	.5293 16	.5542 19	.3734 70	.1734 40	.6137 52	.6306 30	.6319 47			
3650	.6127 09	.5470 15	.5133 12	.4077 30	.2409 28	.0531 22	.1499 22	.1653 42	.1740 28			
3663	.1603 22	.0989 22	.0581 33	.6274 44	.4725 39	.2789 36	.6663 56	.6845 27	.6814 49			
4046	.4451 12	.3877 09	.3555 18	.9760 21	.8343 09	.6629 21	.8441 33	.8571 19	.8547 22			
4077	.0254 12	.9631 47	.9381 27	.5593 42	.3999 46	.2424 15	.0361 43	.0423 53	.0431 31			
4358	.3669 21	.3179 27	.2899 09	.9781 07	.8393 24	.6837 28	.0804 42	.0994 18	.0961 10			
5460	.7073 13	.6708 19	.6432 21	.1205 18	.0137 31	.8931 21	.6077 18	.6183 19	.6160 15			

* Except Plate 14, 2t = 5.000 179 cm.
Standard deviations indicated are in
the last two figures of the fractions.

TABLE IX. Observed Refractivities*

Vacuum Wavelengths	(n - 1) x 10 ⁶ ; using plates										Final Mean
	1, 11	2, 12	3, 13	4, 14	5, 15	6, 16	7, 17	8, 18	9, 19		
	1.5 cm. etalon			2.5 cm. etalon			2.8 cm. etalon				
6268.23	276.490	276.623	276.531	276.475	276.431	276.429	276.399	276.500	276.424	276.460	
6219.00	276.553	276.616	276.587	276.606	276.570	276.630	276.581	276.569	276.556	276.585	
5946.48	276.856	276.874	276.759	276.929	276.852	276.835	276.908	276.859	276.894	276.863	
5854.11	277.008	277.051	277.027	277.029	277.134	277.196	277.160	277.118	277.196	277.102	
5462.27	277.939	277.913	277.765	277.782	277.787	277.627	277.906	277.828	-	277.830	
4359.56	280.983	280.946	281.089	280.960	280.961	280.986	280.808	280.918	280.879	280.948	
4078.99	282.195	282.016	282.229	282.331	-	282.233	282.165	282.165	282.167	282.193	
4047.71	282.325	282.314	282.367	282.389	282.402	282.413	282.425	282.389	282.371	282.377	
3664.32	284.992	284.729	284.521	284.741	284.784	284.750	284.774	284.774	284.723	284.754	
3651.20	284.773	284.779	284.895	284.767	284.795	284.750	284.668	284.813	284.921	284.796	
3342.44	287.342	287.453	287.318	287.557	287.379	287.451	287.324	287.307	287.419	287.374	
3126.58	289.723	289.751	289.759	289.760	289.858	289.877	289.640	289.786	289.549	289.756	
3022.38	291.140	291.180	290.470	291.202	291.167	291.178	290.930	291.067	291.030	291.048	
2968.15	291.894	291.839	291.920	291.980	291.896	291.940	291.692	291.873	291.808	291.881	
2894.45	292.921	293.053	292.949	293.154	292.931	292.977	293.022	293.077	292.969	292.987	
2753.60	295.562	295.574	295.690	-	-	295.555	295.501	295.621	295.422	295.563	
2652.83	297.670	297.426	297.623	298.028	297.410	297.427	297.325	297.566	297.651	297.627	
2537.21	300.273	300.407	300.228	300.397	300.421	300.460	300.300	300.406	300.231	300.367	

* All values corrected to the same conditions of temperature and pressure.

TABLE IXa. Comparison of Observed and Calculated Values of Refractivity.

Vacuum Wavelengths	$(n-1) \times 10^6$			(B)-(A)	(C)-(A)
	(A) Observed Mean	(B) Calculated using eq.(25)	(C) Calculated using eq.(28)		
6268.23	276.460	276.504	276.469	+ 0.044	+ 0.009
6219.00	276.585	276.568	276.535	- 0.017	- 0.050
5946.48	276.863	276.949	276.923	+ 0.086	+ 0.060
5854.11	277.102	277.091	277.068	- 0.011	- 0.034
546.27	277.830	277.782	277.771	- 0.048	- 0.059
4359.56	280.948	280.914	280.938	- 0.034	- 0.010
4078.99	282.193	282.184	282.213	- 0.009	+ 0.020
4047.71	282.377	282.343	282.372	- 0.034	- 0.005
3664.32	284.754	284.685	284.722	- 0.069	- 0.032
3651.20	284.796	284.779	284.811	- 0.017	+ 0.015
3342.44	287.374	287.393	287.416	+ 0.019	+ 0.042
3126.58	289.756	289.769	289.781	+ 0.014	+ 0.025
3022.38	291.048	291.131	291.136	+ 0.083	+ 0.088
2968.15	291.881	291.907	291.908	+ 0.026	+ 0.027
2894.45	292.987	293.043	293.000	+ 0.066	+ 0.013
2753.60	295.563	295.526	295.509	- 0.037	- 0.054
2652.83	297.627	297.597	297.573	- 0.030	- 0.054
2537.21	300.367	300.347	300.322	- 0.020	- 0.045

TABLE X. Pressures and Temperatures.

Plate	Temp. in Degrees Centigrade	Pressure in mm. of mercury				
		Initial Neon	198. 80 Hg. Visible	198. 80 Hg.-2536	198. 80 Hg. Ultra violet	Final Neon
11	21.393	758.57	758.58	758.68	758.77	758.92
12	21.398	756.36	756.46	756.59	756.73	756.93
13	21.397	755.30	755.34	755.44	755.54	755.74
14	21.398	757.91	757.95	758.04	758.12	758.27
15	21.399	760.52	760.66	760.70	760.95	761.16
16	21.396	756.56	756.64	756.76	756.94	757.28
17	21.396	758.30	758.41	758.59	758.75	758.95
18	21.397	758.46	758.51	758.65	758.80	759.03
19	21.398	758.36	758.30	758.44	758.56	758.72

Bibliography

- (1) Fabry and Buisson, *Astrophysics J.* 28, 169, (1908)
- (2) Newbound, *J. Opt. Soc. Am.* 39, 835, (1949)
- (3) Meggers and Peters, *Bull. of the Bur. of Standards*, 14, 697, (1918)
- (4) Kosters and Lampe, *Physik. Zeits.*, 35, 223, (1934)
- (5) Perard, *Trav. Bur. Int. Pds. Mes.*, 19, 78 (1934)
- (6) Barrell and Sears, *Phil. Trans. Royal Soc.*, 238, 1, (1939-40)
- (7) Meggers and Kessler, *J. Opt. Soc. Am.* 40, 737, (1950)
- (8) Edlen, *J. Opt. Soc. Am.*, 43, 339, (1953)
- (9) Koch, *Arkiv, Mat. Astron. Fysik*, 8, No. 20, (1912)
- (10) Traub, *Ann. Physik*, 61, 533, (1920)
- (11) Meissner, *J. Opt. Soc. Am.*, 31, 405, (1941)
- (12) Tolansky, *High Resolution Spectroscopy*, Methuen, (1947)
- (13) Smith, "Precision Determination of Argon wavelengths in the region 3900 A to 4600 A", Unpublished Masters Thesis, Library, University of Alberta, (1952)
- (14) M.I.T. Radar School Staff, *Principles of Radar*, McGraw-Hill, (1948)
- (15) Olafson, "Ultra Violet Dispersion of Air", Unpublished Masters Thesis, Library, University of Alberta, (1955)
- (16) *Handbook of Chemistry and Physics*, 32nd edition, Chemical Rubber Publishing Company
- (17) Palmer, *Theory of Measurements*, McGraw-Hill, (1912)
- (18) Kenney and Keeping, *Mathematics of Statistics*, 2nd edition, Van Nostrand, (1951)
- (19) Ditchburn, *Light*, Blackie and Sons Ltd., (1952)
- (20) Schultz, "Precision Determination of Wavelengths in the Spectrum of Mercury 198", Unpublished Masters Thesis, Library, University of Alberta, (1956)

ACKNOWLEDGEMENTS

Appreciation is expressed to Dr. K. B. Newbound who suggested the topic for research and directed the work. Dr. Newbound offered many helpful suggestions during the course of the investigation and also assisted with some of the many tedious calculations.

Thanks are also due Dr. D.B. Scott for his aid and encouragement, and A. A. Schultz who helped during the experimental phase of the work and who determined the partial orders of interference for all vacuum exposures.

The work was supported by grants from the National Research Council.



